Microchemical Journal 158 (2020) 105121

Contents lists available at ScienceDirect

Microchemical Journal

journal homepage: www.elsevier.com/locate/microc

A multi-analytical approach for the characterization of black crusts on the facade of an historical cathedral

Valeria Comite[a,*], José Santiago Pozo-Antonio[b], Carolina Cardell[c], Luciana Randazzo[d], Mauro Francesco La Russa[d], Paola Fermo[a]

[a] Dipartimento di Chimica, Università degli Studi di Milano, Via Golgi 19, Milan, Italy
[b] Departamento de Enxeñaría de Recursos Naturais e Medio Ambiente, Escola de Enxeñaría de Minas e Enerxía, University of Vigo, Campus Lagoas-Marcosende s/n, 36310 Vigo, Spain
[c] Department of Mineralogy and Petrology, Faculty of Science, University of Granada, Av, Fuentenueva S/N, 18002 Granada, Spain
[d] Dipartimento di Biologia, Ecologia e Scienze della Terra (DiBEST), Università della Calabria, Via Pietro Bucci, 87036 Arcavacata di Rende, CS, Italy

ARTICLE INFO

Keywords:
Black crusts
Marble stone
Cultural heritage
Conservation
Black carbonaceous particles
Urban air pollution

ABSTRACT

This study focuses on the characterization of black crusts collected from the Monza cathedral located in the homonymous city (N Italy), a hot spot from the point of view of the atmospheric pollution. Black crusts and substrate marble specimens were analyzed by a multi-analytical approach including X-ray Diffraction (XRD), Fourier Transform-Infrared spectroscopy (FT-IR), Stereomicroscopy (SM), Polarized Light Microscopy (PLM), High Resolution Scanning Electron Microscopy coupled with Energy Dispersive X-ray spectroscopy (HRSEM-EDX) and Laser Ablation Inductively Coupled Plasma Mass Spectrometry (LA-ICP/MS). The characterization of the carbon fraction (organic carbon, OC, and elemental carbon, EC) was performed using a new approach based on the use of Carbon Hydrogen Nitrogen (CHN) analysis and Thermogravimetric Analysis (TGA). The integrated approach allowed the identification of the pollution sources responsible for black crusts forming process. The precise identification of the main substances responsible for the surface degradation phenomena, in particular those leading to the blackening and disintegration of the carbonate substrates, is essential for the definition of conservative intervention and maintenance strategies, as well as for the development of emission reduction policies on a local scale.

1. Introduction

Atmospheric pollution (such as gases and particulate matter) interacts with stone materials and generates various typologies of decay [1–5]. Among those we can list, for instance, salt crystallization that can lead to physical stress or soiling that may evolve to black crusts (BCs hereafter) when in presence of humidity and absence of water washout processes [6–8]. The formation of BCs is one of the most dangerous phenomenon in architectural heritage [9–11]. Currently, emissions from mobile combustion sources [12–14] are the main agents responsible for air pollution in cities, although a significant decrease is expected in the next years, due to reinforced pollution prevention law and policies. Especially the monuments located in the historic centres of large cities are subjected to typical anthropogenic emissions. Sulfur dioxide, despite its decreasing concentration emitted in the atmosphere, is the main specie responsible for sulfation process that occurs on the stone [15–22]. Up to now, BCs have been the subject of numerous studies [10,23,24] which highlighted the importance of investigating this topic in order to study physical–chemical decay of stone surfaces [25–30]. BCs formation is not only a form of alteration of carbonate stones but also of other types of rock such as granite [22,31,32].

It is generally recognized that there is a correlation between the chemical composition of BC and air pollution [33–40]. The composition of the surface deposits on the stone (dust, BCs) could be used as an indicator of environment and climate change [39]. Furthermore, numerous publications have highlighted the importance of deepening the knowledge of the degradation products because they lead to physical–chemical decay and also act as an accumulator of pollutants [10,23,25–28].

Starting from this scientific overview, this study is based on the characterization of BCs taken from the historical cathedral of Monza (dating to 14th century), placed in a polluted urban centre in the North

* Corresponding author at: Dipartimento di Chimica, Università degli Studi di Milano, Via Golgi 19, Milan, Italy.
E-mail addresses: valeria.comite@unimi.it (V. Comite), ipozo@uvigo.es (J.S. Pozo-Antonio), cardell@ugr.es (C. Cardell), luciana.randazzo@unical.it (L. Randazzo), mlarussa@unical.it (M.F. La Russa), paola.fermo@unimi.it (P. Fermo).

https://doi.org/10.1016/j.microc.2020.105121
Received 3 September 2019; Received in revised form 1 June 2020; Accepted 1 June 2020
Available online 03 June 2020
0026-265X/

of Italy. The cathedral is located in the homonymous city placed ca. 20 km NE of Milan. Monza covers an area of 33.09 km^2 and has 123.776 inhabitants and is the third largest city in the Lombardy region (Northern Italy) [41]. The city suffers from high pollution produced by intense vehicular traffic, use of domestic heating, as well as pollution produced by industrial and agricultural activities typical of the Po Valley. In Monza, NO_X emissions are due mainly to traffic (69%) but are also to domestic heating (12%), industries (12%) and incinerators (3%) while anthropogenic VOC (volatile organic compounds) emissions are linked to the use of solvents (69%) and to traffic (9%). NH_3 emissions on a regional scale are due to agriculture and breeding activities. The percentage values listed are higher than those recorded for the city of Milan. Moreover, in spite of SO_2 reduction recorded during the last years, for the city of Monza this pollutant is due to industrial activity for 82% (as reported in INEMAR, INventario EMissioni Aria, ARPA Lombardia 2014), the presence of SO_2 still dominates the chemical composition of the deposits in urban environments.

The samples analyzed in this work were taken from the facade of the Monza cathedral (Basilica of San Giovanni Battista) located in Monza in the homonym square (Fig. S1 in Supplementary material). The façade, a remarkable example of 14^{th} century architecture, and divided into three parts, was designed and finished by Matteo da Campione between 1300 and 1350; it is characterized by alternating dark and white-colored rows of stone blocks. From the 18^{th} to the 20^{th} centuries several and complexes restoration interventions followed that involved some areas of the façade [42]. The dark and white-colored degraded rows were replaced with new ones, all the missing columns of white marble integrated, and the rose window was consolidated. Furthermore, some elements of the three-light windows and the quadrangular compartments on the black background of the rosettes in the central area were restored. In the final phase, a cleaning restoration was performed in the lower central and upper part of the façade. In 2017 the façade was restored once again.

BCs sampled from the cathedral façade studied in the present work, have developed on the different marbles used for the monument construction. In order to completely characterize the samples, several analytical techniques were used such as: XRD (X-ray Diffraction), FT-IR (Fourier Transform-Infrared spectroscopy), SM (Stereomicroscopy), PLM (Polarized Light Microscopy), HRSEM-EDX (High Resolution Scanning Electron Microscopy coupled with Energy Dispersive X-ray spectroscopy), LA-ICP/MS (Laser Ablation Inductively Coupled Plasma Mass Spectrometry) CHN (Carbon Hydrogen Nitrogen) and TGA (Thermogravimetric Analysis). This integrated approach has allowed us to gain information about the composition (chemical and mineralogical) and texture of the BCs making it possible to identify the pollution sources causing the stone decay, as well as the variability in BC composition depending both on the exposure conditions of the analyzed crust surfaces and their estimated age. In this sense, the older crusts should be present on the original marbles and crusts of more recent formation should have evolved on new marbles used during the cathedral restoration.

2. Materials and analytical methods

2.1. Sampling

During the last restoration carried out in 2017, 9 samples of BCs developed on marble stones, were taken from the cathedral façade at different heights (Fig. S2) following the indications of the restorers. The facade of the cathedral of Monza is oriented to North-West side which is the most exposed to the atmospheric agents (rain, winds, etc.) and corresponds to the lateral nave. The BCs samples were all taken inside the architectural frames of windows and oculi (i.e. small circular openings) in areas protected from rainwater or runoff. The samples show variable color (dark grey and black), morphology (linear compact and dendritic) and thickness, depending on the exposure position and on textural features of the underlying substrate.

Two groups of BCs were identified, group A and group B (Fig. 2S), according to the information available on restoration interventions in the specific areas from where they were taken:

- group A is formed by BC samples 1MD, 3MS and 4MS located at ca. 16 m high, and taken from the area restored by Conca (original marbles replaced in 1735); therefore, these crusts are estimated to be about 280 years old, consequently pollutants accumulation of about 280 years was present;
- group B is formed by BC samples taken from a height of ca. 12 m, i.e. 5MC, 7MD, 8MD and 9MS, and BC samples 11MD and 12MD taken at ca. 5 m height (lower part of the façade) in areas that have never been restored therefore, these crusts are about 650 years old, i.e. 650 years of pollutants accumulation.

It is worth to noting that also in the literature [13,28,35,36,43-45] it is attested that dating of BCs can be performed on the basis of the period of pollutants accumulation.

The sampling points were chosen according to the advice of the director of the restoration works and his team, who clearly distinguished the BCs growth on the original marbles from the BCs developed on the substituting (new) marbles. Their indications are proven by documents (unpublished) present in the cathedral archives that have made it possible to confirm these deductions. Furthermore, the sampled BCs did not show surface detachment phases (a phenomenon that is present in the case of restored surfaces) and were positioned within the architectural frames of windows and oculi (i.e. small circular openings) in areas protected from rainwater or runoff. The architectural frames have also protected the sampled areas over time.

A brief sample description accompanied by information regarding BCs sampling point, height and information on eventual previous restorations is summarized in Table 1. The BC samples were named on the basis of their position on the facade (M = Monza; D = right; C = center; S = left). BC samples were divided into different aliquots and analyzed.

2.2. Analytical methods

2.2.1. Stereomicroscope (SM)

A stereomicroscope (SMZ 1000, Nikon, Japan) equipped for microphotography was used to look at the chromatic and textural features, as well as the conservation state of the BCs and their marble substrates studied as chip (bulk) samples.

2.2.2. Polarized Light Microscopy (PLM)

Mineralogical composition, texture, microstructure and conservation state of the BCs and the marble substrates were studied by Polarized Light Microscopy (PLM) in transmitted and reflected light using a Carl Zeiss Jenapol U instrument (Germany) with a digital camera (Nikon D-7000). To this end the chip samples were prepared as polished thin sections to study their cross sections.

2.2.3. X-Ray Diffraction (XRD)

Mineralogical composition of the BCs was obtained by means of XRD (Siemens D5000) according to the random powder method. BCs were separate from the substrate with a hammer and a chisel and then, they were ground to a fine powder in a mechanical ball mill. In the diffractograms obtained, relative abundance (semi-quantitative estimation) was determined for each mineral phase using the area of highest-intensity diffraction peaks and the intensity ratios established from artificial mixtures of standard minerals [46].

2.2.4. Fourier Transform Infrared Spectroscopy (FT-IR)

In order to complete the information given by XRD, the chemical composition of the BCs (ground samples) was characterized using FT-IR

Table 1
List of BC samples collected from the façade of the cathedral of Monza.

	Sample	Height and location	Description	Stone	Years of Pollutants accumulation
Group A	1MD	16 m rose window right side of the façade	Black crust on marble	The stone is a later integration (1735 year)	About 280
	3MS	16 m rose window left side of the façade	Black crust on marble	The stone is a later integration (1735 year)	
	4MS	16 m rose window left side of the façade	Black crust on marble	The stone is a later integration (1735 year)	
Group B	5MC	12 m rose window central part of the façade	Black crust on marble	Original	About 650
	7MD	12 m rose window right side of the façade	Black crust on marble.	Original	
	8MD	12 m rose window right side of the façade	Black crust om marble	Original	
	9MS	12 m left double-arched window, original capital of the façade	Black crust on original marble	Original	
	11MD	5 m double-arched window, right side of the façade	Black crust on original marble	Original	
	12MD	5 m double-arched window, right side of the façade	Black crust on original marble	Original	

spectroscopy (Thermo Nicolet 6700) in Attenuated Total Reflectance (ATR) mode. Functional groups in the absorbance spectra for each sample were identified. XRD and FT-IR used together allowed a complete mineralogical composition of the BCs.

2.2.5. High Resolution Scanning Electron Microscopy coupled with Energy Dispersive X-Ray Spectroscopy (HRSEM-EDX)

The micro-texture and chemical composition of the BCs and marbles substrates were analyzed using a HRSEM-EDX. The instrument was a Supra 40Vp Carl Zeiss (Germany) furnished with BSE (backscattered electrons) and SE (secondary electrons) detectors (InLens) that deliver chemical and morphological images respectively, as well as a micro-analysis system (Aztec 3) to provide elemental analyses by EDX (X-Max 50 mm detector). Bulk (chip) samples (to analyze the BC surface) and polished thin sections (to study the sampleś cross section) were mounted on Al stubs with double-sided adhesive C tape and carbon coated. Samples were analyzed under high vacuum level. EDX single-point analyses were acquired from different points of interest (5 to 10 single-point analyses for each point) either from bulk or polished thin sections at 10 kV (bulk samples) and 20 kV beam energy (thin sections). High-resolution X-ray maps (1024 × 768 pixels, 10 ms dwell time, 2.5 h acquisition, 20 eV/ch resolution, and 43–1000 frames) were obtained from selected areas (thin sections) by compiling elemental distribution maps through the use of the *Find Phases* tool implemented in the Aztec 3 EDX. This allowed us to highlight the amount, location and morphology of crystalline/amorphous phases present in the samples.

2.2.6. Laser Ablation Inductively Coupled Plasma Mass Spectrometry (LA-ICP-MS)

BCs as well as chemical analyses in terms of trace elements were performed by LA-ICP-MS. This method allowed us to investigate a great number of elements with spot resolutions of about 40–50 μm, and to determinate micrometric compositional variations [47–49]. Analyses were carried out using an Elan DRCe instrument (Perkin Elmer/SCIEX) connected to a New Wave UP213 solid-state Nd-YAG laser probe (213 nm). The number of analyses carried out on the samples were related to the BC thickness, in particular ranging from three to five-point analysis. The analytical procedure to characterize the BCs is well established in varied studies in the literature [23,43,44,50].

2.2.7. Carbonaceous fraction analysis

For quantifying the carbonaceous components present in the BCs, Carbon Hydrogen Nitrogen (CHN) analyses were performed by a CHN analyser (CHNS/O Perkin Elmer 2400 Series II Elemental Analyzer using an accessory for the analysis of solids). Thermogravimetric analyses (TGA) were carried out by a Mettler Toledo TGA/DSC 3 + instrument which allows simultaneous TG and DSC (Differential Scanning Calorimetry) analyses. The analyses were conducted in the range 30–800 °C, increasing the temperature with a rate of 20 °C/minute. The carbonaceous components were estimated considering their temperature range decomposition previously defined analyzing standards and using two different atmospheres, i.e. the inert and the oxidant one. Before performing the analyses, the BCs samples were separated from the marble substrate (using a scalpel) and ground in an agate mortar. The power samples were analyzed only once due to the limited quantity of the sample. The uncertainty of the technique has been previously evaluated together with the limit of detection [51,52].

3. Results

3.1. SM, PLM, XRD and FT-IR analysis

The stereomicroscope (SM) study revealed that all BCs samples exhibit intense black color on surface (except 1MD), though their thickness and surface features vary depending on location and height of sampling in the building. For instance, 12MD sample taken at 5 m high

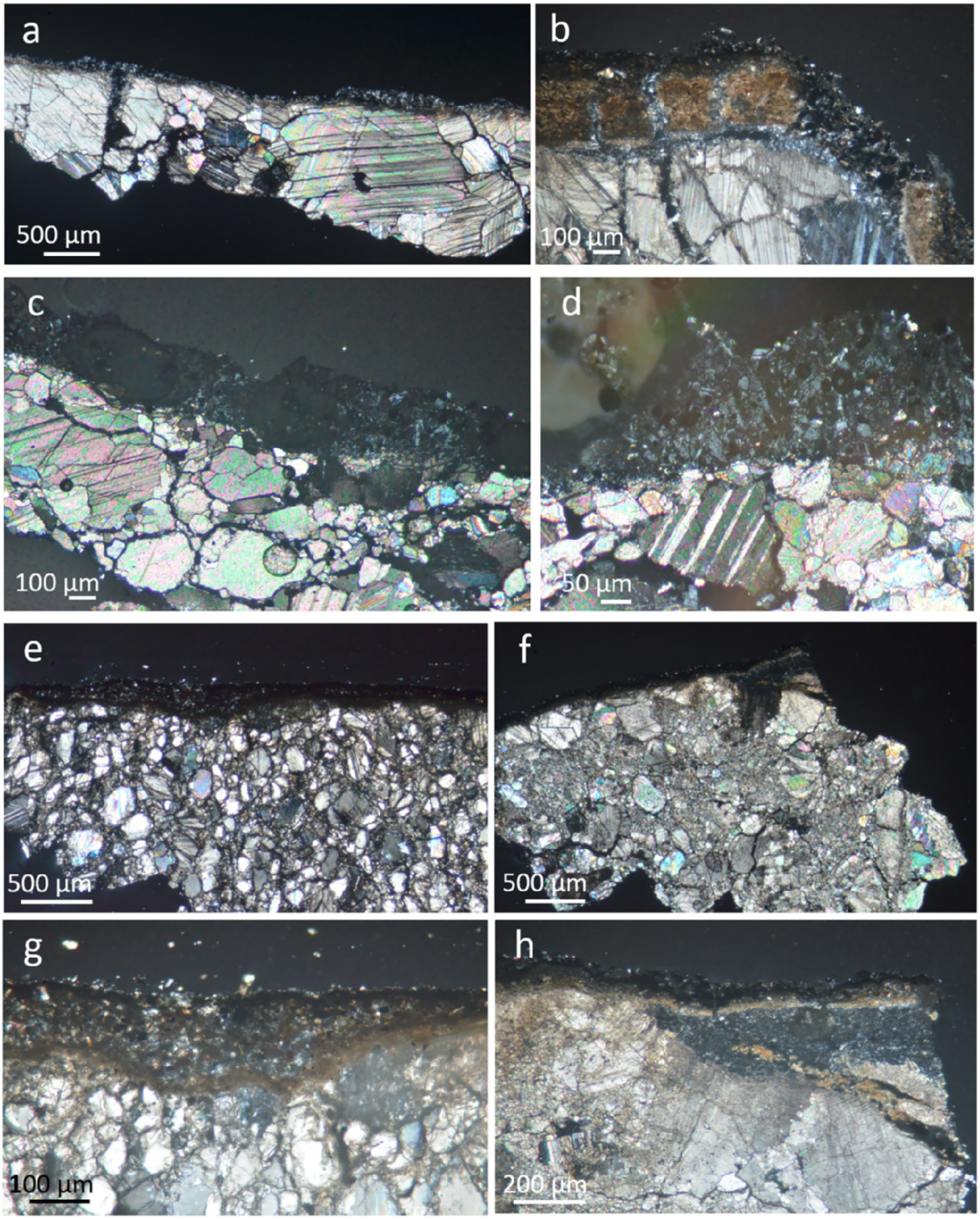

Fig. 1. Microphotographs of BCs samples (thin sections) from cathedral of Monza taken with PLM (crossed polars). a) 1MD (16 m high), note the large crystal size and the gypsum crystals filling the calcite crystals fissures; b) 12MD (5 m high), note the intense fissure system of the marble, the 3 layers of the crust and the abundant BCPs; c and d) 4MS (16 m high), note the heteroblastic fabric of the marble and the small calcite crystals fragments being incorporated into the gypsum crust; e) 7MD and f) 9MS (12 m high), note the dissimilar marble substrates highly fractured; g) 7MD and h) 9MS, note the orange-brown layer in contact with the marble. BCPs = Black Carbonaceous Particles.

is made of 3 layers as clearly seen in Fig. S3a in Supplementary Material (indicated in the red rectangle); the one in contact with the substrate is orange-brown, on top there is a white layer and above a black layer. Some crusts clearly show particles of different color (white, red and grey) on their surface such as 7MD, 1MD and 11MD samples, these two last displaying uneven surface continuity (Fig. S3b–d).

The PLM study confirmed that all crust substrates are marbles, however exhibiting diverse petrographic characteristics in that marbles are of different types. Fig. 1 shows the marked microstructural differences in terms of crystal size, shape and grain boundaries. Note that all marbles are physically degraded presenting varied damage degree. 1MD and 12MD marbles exhibit granoblastic-heteroblastic fabric and mosaic type distribution of polygonal cleavage crystals forming triple junctions at 120°. 1MD displays the largest crystal size ranging from ca. 0.2 to 1.4 mm (Fig. 1a), while crystals size range from ca. 0.2 to 0.5 mm in 12 MD (Fig. 1b). Fissures and cracks are abundant in both marbles. 4MS marble exhibits heteroblastic fabric. Crystals have sub-angular to rounded shapes and lobate boundaries with sizes

Table 2
Mineralogical composition of the BCs collected from cathedral of Monza. G: gypsum; Q: quartz; C: calcite; WD: weddellite; WW: whewellite. + + + +: > 50%; + + +: 30–50%; + +: 10–30%; +: 3–10%; tr: < 3%. -: not detected.

	Samples	G	Q	C	WD
Group A	1MD	+ + + +	+	–	–
	3MS	+ + + +	+	–	–
	4MS	+ + + +	–	–	tr
Group B	5MC	+ + + +	tr	–	tr
	7MD	+ + + +	+ +	–	–
	8MD	+ + +	+ + +	–	–
	9MS	+ + + +	+	–	+
	11MD	+ + + +	+	tr	–
	12MD	+ + + +	+ +	–	–

ranging from ca. 50 μm to 0.3 mm (Fig. 1c). Note the intense cracking of the substrate and the calcite crystals from the marble substrate embedded in the gypsum matrix of the BC (Fig. 1d). The highly degraded 7MD marble (Fig. 1e) has a microstructure made of rounded crystals with a bimodal size distribution (< 40 μm to 0.3 mm). A porfido-granoblastic fabric characterizes 9MS marble, composed of non-equi-dimensional rounded shaped-grains ranging in size from few microns to 0.4 mm (Fig. 1f). Marble is severely degraded as to develop granular disaggregation.

Gypsum ($CaSO_4{\cdot}2H_2O$) was detected by XRD in all BCs samples as the main mineral phase (Table 2). Moreover, quartz (SiO_2) was detected in all BCs in different amounts, except in 4MS. Other minerals were detected in low amounts: i) weddellite ($CaC_2O_4{\cdot}2H_2O$) was identified in 4MS, 5MC and 9MS (mainly in the latter), and ii) calcite ($CaCO_3$) in 11 MD.

FT-IR analysis confirmed and completed the XRD results; gypsum is the main mineral phase in BCs (Fig. 2). The presence of this mineral is confirmed through the bands assigned to 1) OH functional group related to the hydration state of the mineral and 2) the S-O vibrations. In the first case, the characteristic OH-(H_2O) bands were confirmed by means of the intense doublet at 3520/3401 cm^{-1}, a slight shoulder at 3244 cm^{-1}, two weak bands at 2640 and 2510 cm^{-1} and medium intense bands at 1682/1618 cm^{-1}. Regarding S-O vibration, the sharped band centred at 1102 cm^{-1} assigned to S-O stretching and the lower intense bands at 667, 596 and 460 cm^{-1} corresponding to S-O bending vibration [53–56]. The detection of quartz by XRD is confirmed by FT-IR through a slight shoulder at 1004 cm^{-1}, typically assigned to the asymmetrical stretching vibration of Si—O of quartz [53,57]. With respect to calcium oxalates, note that the discrimination of weddellite and whewellite is made from the bands assigned to the symmetric O—C—O stretching vibrations at 1317 cm^{-1} and 1324 cm^{-1} for whewellite and weddellite respectively [50,58]. In addition, the vibration corresponding to H—O—H vibration of lattice water is detected at 1630 cm^{-1} and 781 cm^{-1} for both oxalates and at 669 cm^{-1} and at 603 cm^{-1} for whewellite and weddellite respectively [50,58]. However, confirmation of the presence of calcium oxalate was only possible in some samples due to two difficulties: 1) the coincidence between the oxalate FT-IR bands between 600 and 700 cm^{-1} with those of gypsum (note that gypsum is the main mineral of all the crusts); and 2) the detection in all BCs samples of a broad shoulder-shaped band around 1370–1400 cm^{-1} that frames the 1317 or 1324 cm^{-1} band of the oxalates. Despite these difficulties, XRD results allowed us to identify this oxalate as weddellite. Therefore, identification of oxalates (weddellite) could be evidenced by FT-IR through the disappearance or smoothing of the doublet at 1681–1619 cm^{-1} of gypsum and its transformation into a wide band nearby these wavenumbers, possibly as a result of the contribution of the 1630 cm^{-1} band (intermediate to double) of weddellite. By means of this doublet modification, the presence of weddellite would be confirmed only in 9MS BC where this oxalate was found in a proportion > 3% by XRD. On the other hand, the FT-IR spectrum of the 8MD BC is striking, since in this sample only gypsum and quartz were detected by DRX. However, the band detected at 1321 cm^{-1} could indicate the existence of calcium oxalate together with the bands at 788 cm^{-1} and 596 cm^{-1}. Calcite, present in trace amounts only in 11MD BC, was identified by means of FT-IR through the FT-IR bands at 1419 and 877, and 713 cm^{-1}. In all the BCs samples, a band around 1400–1370 cm^{-1} is detected; in some cases (1MD, 9MS, 3MS, 7MD, 5MC and 11MD) showing considerable high intensity. This band could be assigned to the symmetric CH_3 bending vibrations and, together with those at 711 and 795 cm^{-1} could indicate the existence of organic matter. Also, the band around 1400–1370 cm^{-1} could be assigned to the asymmetric NO_3 stretching vibrations [53]; this band together with those at 870 and 711 cm^{-1} (characteristic of the bending vibration of NO group) would indicate the presence of nitrate salts.

3.2. HRSEM-EDX and LA-ICP-MS analyses

HRSEM-EDX allowed us to obtain detailed information on crusts' morphologies and their interface with the substrate, as well as information about the chemical composition of the particles present in the BCs. Only a few representative samples of group A (1MD and 4MS) and B (7MD, 9MS and 12MD) were analyzed in this study. In all BC samples the results obtained have shown that the crust (degradation layer) is composed of crystals made of Ca and S (attributed to gypsum) showing different habits for the two BCs groups. Inside the gypsum matrix several particles have been observed showing different chemical composition. In particular, BCs of group B are rich in metal particles. The substrates of all BC samples show intense crack networks (especially BCs of group B), and in some of these cases, microcrystalline gypsum has been observed.

LA-ICP-MS analysis allowed us to determine the trace elements (average concentrations in ppm) related to representative BCs samples (Fig. 3a, b); in particular, the criteria chosen were: different accumulation time of pollutants, height and location of the BCs on the façade of the cathedral (right and left).

Results about trace elements suggest concentration especially for some metals such as: As, Ba, Cd, Cu, Fe, Mn, Ni, Pb, Sb, Sn, Sr, V, and Zn, in agreement with the HRSEM-EDX results. In general the data underline that BCs placed at a lower height and with a greater period of accumulation of pollutants (about 650 years, group B) show higher contents of heavy metals. On the contrary, BCs samples taken at higher altitude, which have less period of accumulation of pollutants (about 280 years group A) show lower concentrations of heavy metals.

3.3. Carbonaceous fraction analysis (OC and EC)

In-depth analysis of carbon could suggest possible pollution sources that cause BCs formation. Total carbon (TC) is composed of OC (Organic Carbon), EC (Elemental Carbon) and CC (Carbonatic Carbon). In this work CC clearly should derived from the substrate which is a marble, although deposition of carbonate-rich soil dust is also possible. EC is responsible for the black color of the crusts; it has a primary origin and is emitted by combustion processes [59,60]. OC is both of primary origin, emitted by traffic or biomass burning [51,61,62], and of secondary origin; in this case it is mainly formed starting from gaseous precursors such as VOC [59,63,64]. Elemental analysis by CHN allowed the determination of TC within the BCs. Furthermore TGA has been successfully applied in the past to discriminate OC from EC [65]. The analysis by TGA/DCS allowed to quantify carbonate carbon percentage (CC%) while elemental carbon percentage (EC%) has been calculated as described in details in La Russa et al., [28]. The organic carbon percentage (OC%) was obtained by difference (OC = TC – (CC + EC)). Table 3 shows the obtained results of the carbon fraction for the two groups of BCs A and B.

In this study, we have observed higher OC values (on average 3.22 for group A and 4.12 for group B) with respect to EC (on average 0.83

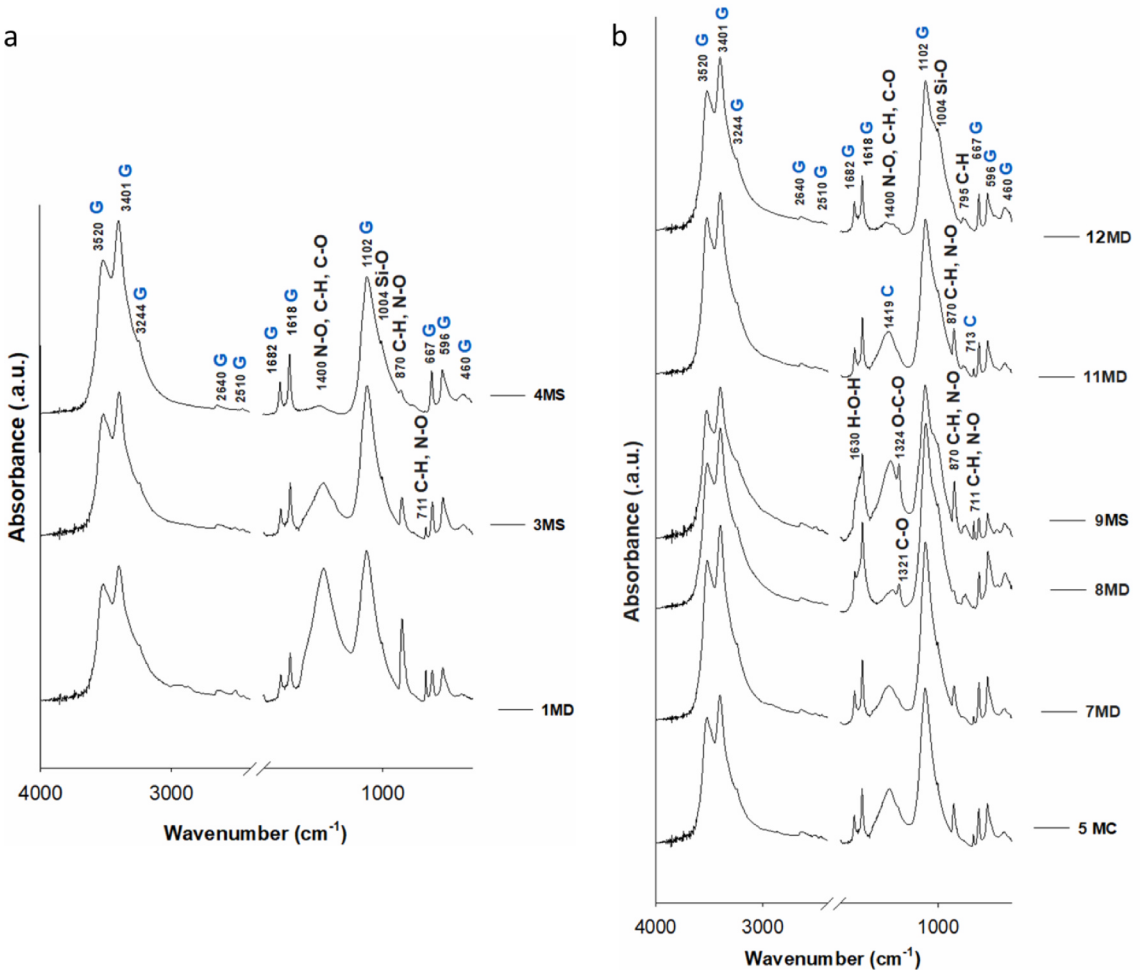

Fig. 2. ATR-FT-IR spectra of the BCs sampled in cathedral of Monza. a) samples belonging to group A. b) samples belonging to group B. Effects assigned to the absorbance bands are depicted and the minerals detected by XRD are shown in blue (G: gypsum, C: calcite).

for group A and 1.02 for group B), in accordance with what happens in the aerosol particulate matter in Milan where OC is the main constituent of TC [52,64–66].

4. Discussion

Samples cross-sections examined with PLM allowed the evaluation of the crust-substrate interface. Regardless of the marble substrate, crusts sampled from the highest altitude (16 m) are made of a single gypsum layer. 1MD (thickness ca. 60–130 μm) is composed of well-developed needle-like gypsum crystals which also fill the marble fissures and cracks near the surface. As Fig. 1a shows, the borders of crystals near the surface are intensely fractured into micrometric grains. Instead, gypsum crystals in 4MS crust display both prismatic and granular habits yielding a thick crust (thickness ca. 145 μm) with copious embedded BCP (Black Carbonaceous Particles) (Fig. 1c, d). BCs are clearly stratified in several layers of different nature, color and thickness in the BCs samples from group B (7MD, 9MD, 12MD see Fig. 1). Here, an orange-brown layer appears at the contact between the substrate and the crust. Similar layers as the one described here have been identified as weddellite by Capittelli et al. [58]. This layer is called *patina noble* [67]. At 12 m high in the building, 9MS (thickness ca. 100–200 μm) and 7MD (thickness ca. 330 μm) BCs exhibit, above the orange-brown layer, a gypsum layer embedding (sub)-spherical BCP in addition to red, yellow and grey particles (Fig. 1g, h). At 5 m height, 12MD BC (thickness ca. 270 μm) show the orange-brown layer which is discontinuous since it is fissured and filled by acicular microcrystalline gypsum crystals (Fig. 1b). The surface of the crust shows intense black color due to the abundant spheroidal BCP (Fig. 1b).

SEM images of bulk 1MD and 4MS (belonging to group A) samples show that crusts are made of an interlocked structure of lenticular and/or hexagonal plate-like crystals arranged as rose-like clusters composed of Ca and S, attributed to gypsum. Fig. 4a is a false-color map based on SEM-EDX elemental mapping of 4MS thin section showing the many fissures of the calcite crystals (from the marble substrate) which are filled by microcrystalline gypsum. Note the copious particles of different nature (e.g. Fe, Si, Mg, Al and Pb) inserted into the gypsum crust matrix. Moreover, as revealed by SEM-SE/BSE analyses, crust contains spherical spongy-like carbonaceous particles (Fig. 4b, c), rounded Fe-rich particles (Fig. 4d, e), Si-rich particles, and cluster of particles where some of the following components were identified, i.e. Pb-chloride, Ca-fosfate, Zn, V, Cr, Co and Br (Fig. 4e, f). Analysis of bulk 7MD, 9MS and 12MD samples (group B) by SEM show that crusts have a powdered texture mostly made of granular and (hexagonal) plate-like gypsum crystals as well as tabular crystals in lesser amount. Spheroidal spongy and/or smooth BCP as well as metal particles are more abundant than in crusts from group A (1MD and 4MS). Analysis of BCs cross sections reveals the intense crack network developed in the marble area in contact with the crusts, particularly severe in samples of group B. Though cracks do not show parallel orientation to the crust surface, they have the potential for physical disintegration (Fig. 5a–d), as proved during handling for microscopic analyses. Fig. 5c shows the dissolution patterns in the calcite crystals and the crystallization of gypsum filling the calcite fissures and cracks. SEM-EDX study has also

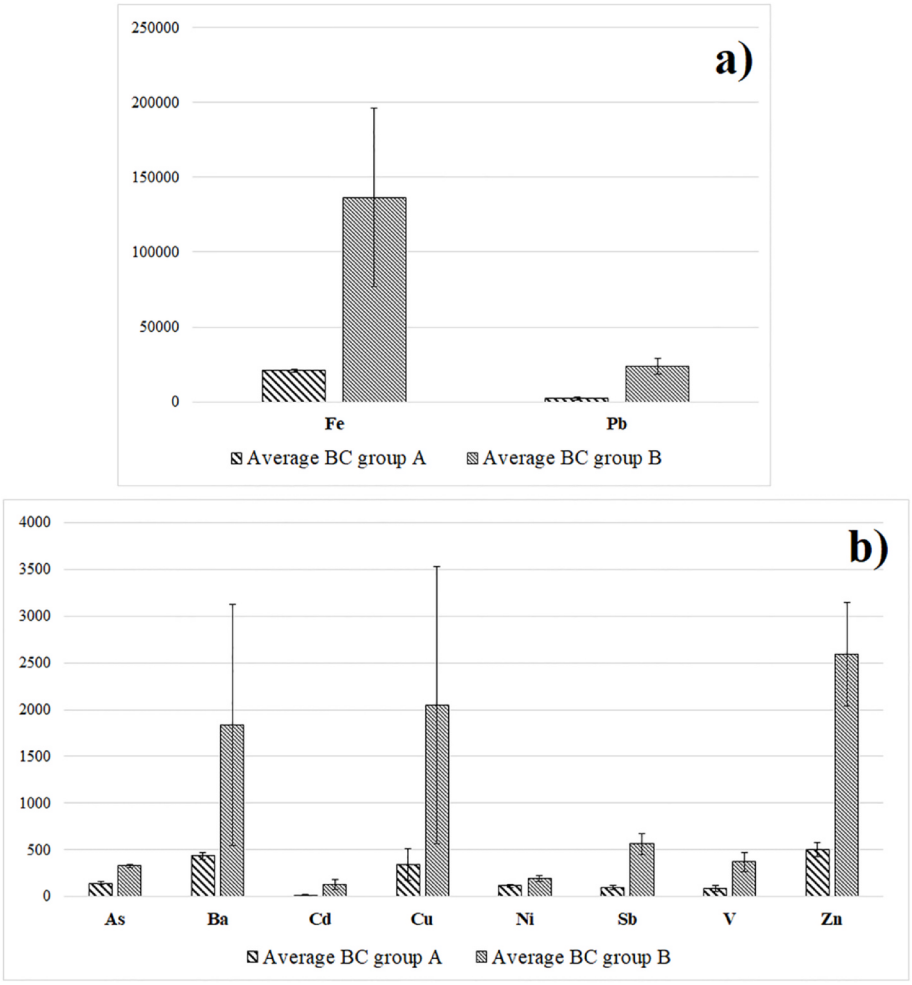

Fig. 3. Histograms showing the average concentrations (in ppm) of heavy metals in BCs of group A and B. a) Fe and Pb; b) As, Ba, Cd, Cu, Ni, Sb, V and Zn.

revealed the numerous metal particles embedded in the gypsum crust matrix in BCs from group B, their morphology and distribution (Fig. S4). In particular, the X-ray map of a selected area in the 7MD sample (Fig. 5b) proves the presence of gypsum, Si-rich, Fe-rich, P-rich and Pb-K-rich particles, these last preferentially located at the marble crust interface. Pb enriched level in the inner zone of crusts has been reported elsewhere [43,45], probably due to the affinity of Pb with calcite from the carbonate substrate.

XRD and FT-IR results allowed to identify that BCs are composed mainly by gypsum as result of the wet or dry deposition of atmospheric sulfur [68] and the subsequent sulfur reaction with the calcium from the marble, regardless of the age of the BC (groups A and B). Despite the most important source of sulfur is SO_2 emissions from fossil fuels, also biological activities and construction materials (mortars and concrete) could contribute to BCs formation [21,32,69–72]. In addition, BCs belonging to group B (650 years old) showed higher quantities of calcium oxalates, since 9MS (mainly), 8MD and 5MC showed weddellite. In samples belonging to group A (280 years old), only traces of this mineral were found in 4MS. Capittelli et al. [58] also identified a mixture of calcium oxalate (both weddellite and whewellite) and gypsum in

Table 3
CC (Carbonate Carbon), EC (Elemental Carbon), OC (Organic Carbon), OX (Oxalate) and TC (Total Carbon) concentrations (wt%) of the collected BCs. Some significant ratios for the analyzed BCs are shown. Average values and standard deviations (wt%) were determined for group A and B.

Sample	CC_{TGA}%	EC_{TGA}%	$(EC + CC)_{TGA}$%	OC%	OX_{TGA} %	TC_{CHN} %	OC/EC	EC/TC
1MD	3.32	0.79	4.19	3.25	0.08	7.44	4.09	0.11
3MS	3.52	0.53	4.11	5.73	0.16	9.84	10.81	0.05
4MS	1.48	1.18	2.73	0.69	0.16	3.42	0.58	0.37
Average BC group A	2.77	0.83	3.68	3.22	0.13	6.90	5.16	0.18
St.dev	0.65	0.19	0.47	1.45	0.03	1.87	3.00	0.10
5MC	3.67	0.37	4.09	4.53	0.05	8.62	12.18	0.04
7MD	3.85	1.04	4.93	4.21	0.11	9.14	4.06	0.11
8MD	2.50	2.32	4.93	1.94	0.27	6.87	0.84	0.37
9MS	4.42	1.05	5.73	5.04	0.15	10.77	4.79	0.10
11MD	3.94	0.79	4.88	4.87	0.1	9.75	6.19	0.08
12 MD	3.57	0.53	4.87	4.10	0.17	8.97	3.43	0.13
Average BC group B	3.66	1.02	4.91	4.12	0.14	9.02	5.25	0.14
St.dev	0.26	0.28	0.21	0.46	0.03	0.53	1.15	0.05

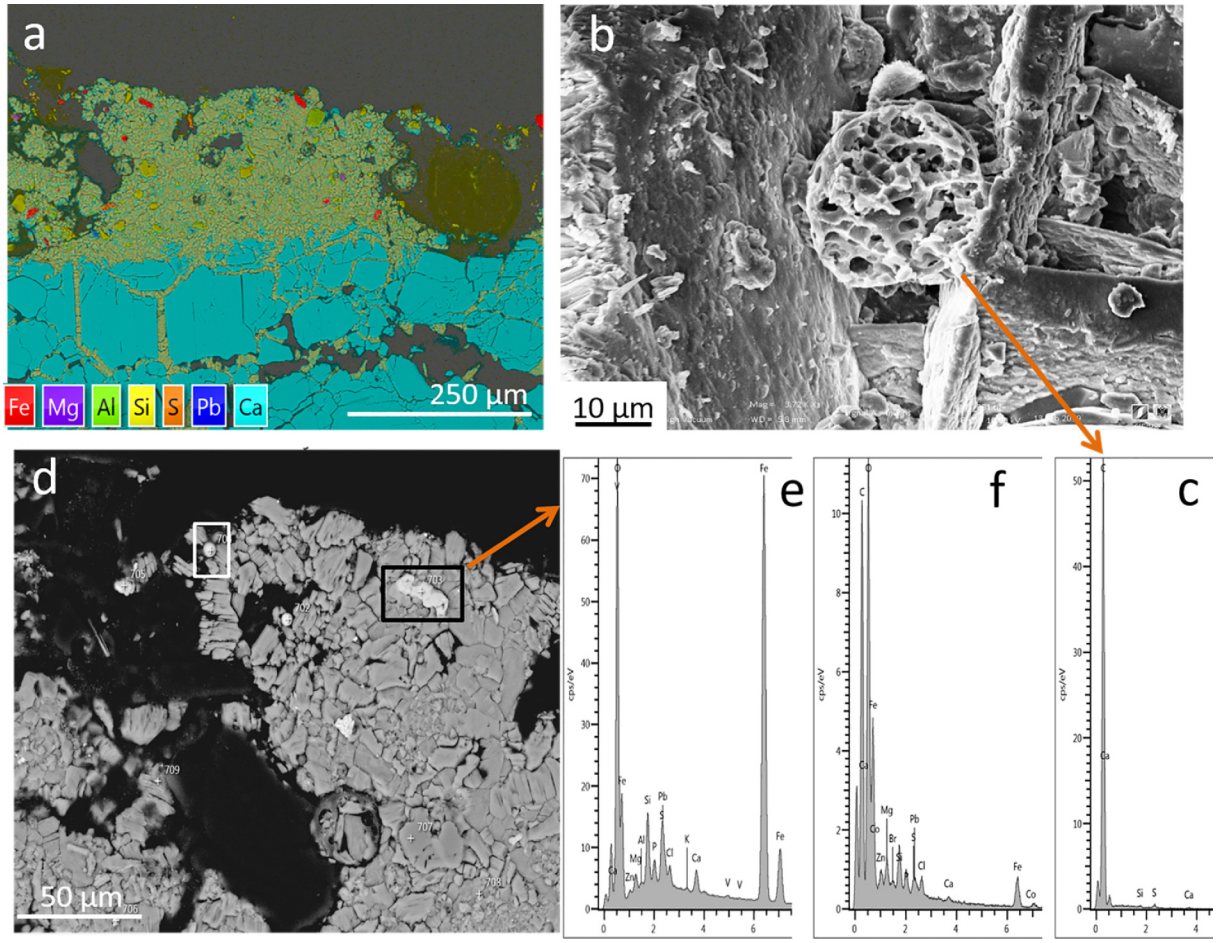

Fig. 4. SEM images showing the BC of 4MD sample: a) SEM-EDX false-color mineral map (thin section); note the significant fissure system of the marble -filled by gypsum- originating granular disaggregation, and the particles of varied nature enclosed into the BC, such as Fe-, Pb-, Si-, and Ca-rich particles; b) spherical spongy-like carbonaceous particle; c) EDX spectrum of carbonaceous particle shown in b); d) BSE-SEM image showing rounded Fe-rich particles (white box) and cluster of metal particles (black box); e) EDX spectrum of white box shown in d; f) average EDX spectrum of the black box shown in d).

yellow-ochre layer on marble of the Milan Cathedral (Italy). As was also found in our samples, Capittelli et al. [58] reported the presence of organic matter and calcite in their patinas. As was indicated by other authors [73,74], calcium oxalates can be formed via biological activity of organisms and reactions of organic compounds in rain or aerosols with the stone. According to literature formation of oxalates can be also due to the application of substances to preserve the rock surfaces [74]. However, having looked carefully at the BCs thin sections and not having detected a continuous layer of oxalate by PLM observations, we can suppose a biological origin.

Higher values of TC and OC (see Table 3) have been found for BCs from group B which were formed on original marble substrates, since these crusts have more years of pollutant accumulation. A great variability of OC/EC value has been observed within both groups of BCs even if on average this ratio is quite similar. On the contrary EC/TC in case of group A is slightly higher indicating, as expected for the most recent BCs, a major contribution of traffic source.

Different studies have put into relation the OC/EC ratios with possible particulate matter (PM) emission sources [75,76]. Relatively high ratios for biomass burning emissions and lower ratios for vehicular emission are reported in the literature, Seinfeld at al. [77] and Schauer et al. [78,79], have stated that OC/EC ratios in the range 1.0–4.2 are typical for diesel- and gasoline-powered vehicular exhaust while ratios in the range 16.8–40.0 are related to wood combustion even if Saarikoski et al. [80] reported an OC/EC ratio of 6.6 for biomass burning and 0.71 for vehicular emissions.

In the present study OC/EC ratios basically lower than or about 4 (1MD group A; 7MD; 8MD, 9MS and 12MD group B) could suggest the dominance of fossil fuel burning sources (mainly vehicular emissions). As stated earlier, Monza is a city with high vehicular traffic. Values above 5 found on a few BCs samples (3MS, 5MC and 11MD) may indicate a greater contribution of biomass burning used as home heating system in the past. It has been evidenced a preferential accumulation of OC in almost all BCs samples. Furthermore a ratio of OC/EC higher than 2.0 has been associated to the presence of both primary and secondary sources while a higher ratio indicates a higher contribution of secondary organic compounds [81]. In this paper, we observed that out of 9 BCs samples examined 7 (1MD, 3MS, 5MC, 7MD, 9MS, 11MD and 12MS) showed an OC/EC ratios $>$ 1 (between 3.43 and 12.18), suggesting a prevalence of organic carbonaceous species over elemental carbon, confirming the formation of secondary organic compounds [76]. This result evidences, contrary to what we believed in the past, that vehicular traffic is not the only source of pollution that affects monuments exposed in polluted urban environment. As previously mentioned, organic substances have different origins also coming from VOC that can be embedded in the BC. We should point out that about 50% of the organic fraction present in powder deposits collected from marble surfaces in Milan [28] is water-soluble and the presence of these substances can be worrying because contributing to accelerate stone decay. The higher values of OC observed for some BCs samples can be attributed to the effect of the biologic colonization that can develop in some cases on the crusts; in fact, some studies indicate [82–85] that

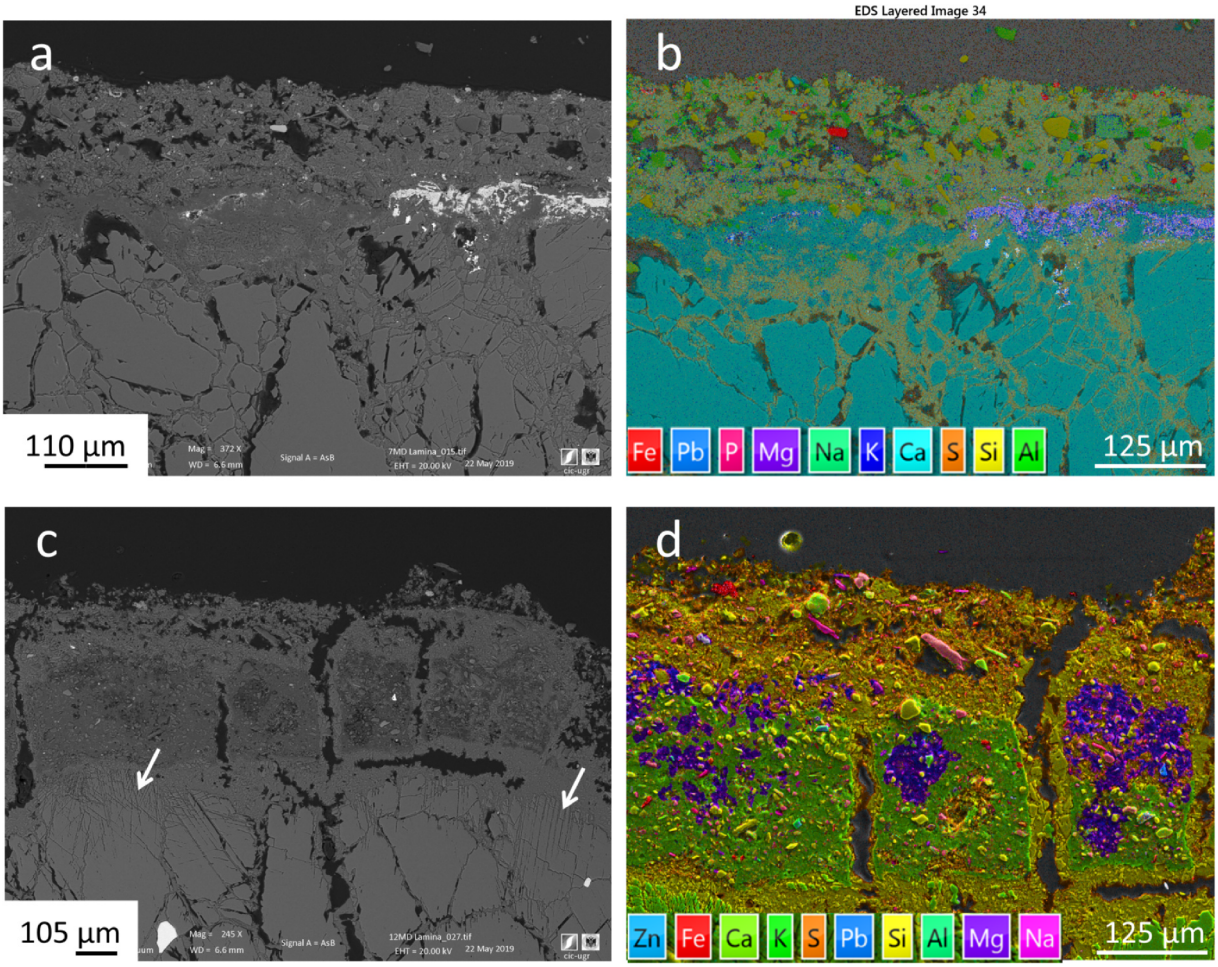

Fig. 5. SEM microphotographs of 7MD and 12MD BCs (thin sections): a) BSE-SEM image of 7MD showing in brighter grey color the copious metal particles; note their accumulation in the interface between the marble and the BC; b) SEM-EDX false-color mineral map of 7MD; note the high amount of Pb and K in the interface marble-crust; c) BSE-SEM image of 12MD revealing the calcite crystals dissolution patterns (arrows) and the structure of the crust which is detaching from the substrate; d) SEM-EDX false-color mineral map of 12MD clearly showing the composition, morphology and distribution of the particles enclosed in the BC.

these processes could create an excess of organic material. Indeed in a recent study, the biological colonization present on the façade of the cathedral of Monza [86] has been highlighted. For example, in sample 3MS (Fig. S5), characterized by a higher OC value with respect to the other BCs samples, this phenomenon was clearly visible. It is also interesting to compare EC/TC ratios with the results obtained for other European cities [29,52,87–90]. In fact, BCs from group A and group B show an average value of EC/TC (0.18 and 0.14 respectively, see Table 3) lower than those observed for the city of Seville (where the same ratio are in the range 0.22–0.36) and Milan (0.5–0.9). Furthermore, BCs collected from cathedral of Monza are influenced by organic substances, probably of secondary origin (because of the high OC/EC ratio).

High CC values detected in group B indicate the greater alteration of the marble substrates as compared to group A. In fact, SEM analyses have shown in these BCs samples the presence of calcite crystals embedded in the gypsum matrix coming from the degraded marble substrate (see Fig. 4a). Calcite was also detected by XRD and FT-IR spectroscopy. TGA allowed the calculation of gypsum percentage in the BCs. It is worth noting that the amount of gypsum is variable (Fig. S6), in agreement with the results obtained with the HRSEM-EDX study. For example, sample 4MS is made mostly by gypsum, while 12MD sample is formed by two well defined layers, being the outermost layer made of gypsum. In addition to the substrate composition as the major influence parameter on the crust development, the cited differences can be caused by different parameters such as the height of sampling, vertical or horizontal position, the exposure to atmospheric agents and the wash out. In fact, the dynamics that are put in motion during the sulfation process are very complex.

Since BCs could be considered as a passive sampler of atmospheric pollution, a deeper investigation of the geochemical features was obtained by measuring the average concentrations of trace elements, using the LA-ICP/MS method. In general, the results are characterized by a certain variability among BC samples. Fe, Pb and Zn are the most abundant elements, while As, Ba, Cd, Cu, Mn, Ni, Sb, Sn and V were always present in a lower amount (in terms of average concentrations).

The graph in Fig. 3a, b shows that the crusts of group B show higher concentrations of trace elements with respect to group A, in particular (Fig. 3a) of Fe (average 136,473 and 20831 ppm for B and A respectively), Pb (average 23,847 and 2055 ppm for B and A respectively) and Zn (Fig. 3b) (average 2595 and 502 ppm for B and A respectively). Differences were also observed (Fig. 3b) for As (average 329 and 114 ppm for B and A respectively), Ba (average 1839 and 435 ppm for B and A respectively), Cd (average 132 and 14 ppm for B and A respectively), Cu (average 2048 and 344 ppm for B and A respectively), Ni (average 191 and 114 ppm for B and A respectively), Sb (average 563 and 98 ppm for B and A respectively) and V (average 370 and 87 ppm for B and A respectively).

In particular, group B shows the highest concentrations of heavy metals, since these BCs were taken from the lower part of the façade, most exposed to vehicular traffic and characterized by a longer pollutants accumulation period. On the contrary, the BCs belonging to group

A show the lower concentration of heavy metals since they were taken from the highest areas not directly exposed to vehicular traffic, and also affected by a lower pollution accumulation period. The heavy metals enrichment observed in BCs from group B is mainly due to the high vehicular traffic that characterizes the city of Monza and the metropolitan area of Milan, although the cathedral has been located in a pedestrian zone in the last decades. However, in the past years, numerous vehicles have been authorized to circulate both in the vicinity and inside the square where the monument is located (see Fig. S1).

In general, all BCs show high contents of Fe, related to emissions from the numerous industries (oil refining, storage, metal extraction and metallurgy, energy production and distribution, and waste incinerator) placed in the near industrial area of Po valley [91,92]. The highest concentrations of Pb, Fe, and Zn observed for BCs of group B are in agreement with the use of lead gasoline [12,93], employed until about 25 years ago. At the same time, Cu, Ni, Cr, and V well match with the use of other combustibles such as: oil combustible, diesel, and gasoline [12,93–97], widespread after the abolition of leaded gasoline.

5. Conclusions

BCs formed on marble stones have been collected from the facade of cathedral of Monza (Italy) and analyzed by several analytical techniques. Two groups of BCs samples were identified, group A and group B, according to the information available on restoration interventions in the specific areas from where they were taken. Petrographic analyses have confirmed that those crusts belonging to group B show a more complex stratigraphy attributable to the greater accumulation time of pollutants compared to BCs of group A, which show a simpler texture. Furthermore, XRD and FT-IR confirm that all BCs are mainly composed of gypsum, with some traces of oxalate and quartz that were detected in different amounts for the different groups; weddellite was mainly found in BCs belonging to the group B (older crusts). The HRSEM-EDX analysis showed that BCs of group B have accumulated more metal particles, mainly Pb-rich particles that are particularly mixed with Cl, which are located in the interface marble-crust due to the affinity of Pb for calcite. Conversely, much less amount of Pb-rich particles are present on the surface of the BCs from group A. Since BCs from group B are closer to the bottom of the building, the impact of vehicle pollution is more evident.

As regards the carbonaceous species (OC and EC), we have demonstrated the preferential accumulation of organic substances in the BCs, probably of the secondary origin or in some cases due to biological contamination.

Significantly different concentration amounts between BCs from group A and B as regards iron, lead, zinc, copper and vanadium have been highlighted, which represent the fingerprint of air pollution occurred in the different years of deposition in the analyzed BCs. In fact, the city of Monza is affected by pollution from the industrial activities, as well as from vehicular traffic.

In conclusion this study confirms the importance of BCs chemical characterization in order to evaluate the actual risk of degradation to which a monument is subjected when exposed to environmental pollution.

CRediT authorship contribution statement

Valeria Comite: Methodology, Validation, Formal analysis, Data curation, Writing - original draft, Writing - review & editing, Project administration, Supervision. **Jose Santiago Pozo-Antonio**: Writing, Formal analysis, Investigation, Writing - review & editing, Supervision. **Carolina Cardell:** Writing, Formal analysis, Investigation, Data curation, Writing - review & editing, Supervision. **Luciana Randazzo:** Investigation, Writing - review & editing. **Mauro Francesco La Russa:** Writing - review & editing, Supervision. **Paola Fermo:** Methodology, Validation, Formal analysis, Data curation, Writing - original draft, Writing - review & editing, Project administration.

Declaration of Competing Interest

The authors declare that they have no known competing financial interests or personal relationships that could have appeared to influence the work reported in this paper.

Acknowledgments

J. Santiago Pozo-Antonio thanks the Spanish Ministry of Economy and Competitiveness (MINECO) for his “Juan de la Cierva-incorporación” (IJCI-2017-3277) contract.

P. Fermo and V. Comite would like to thanks Ing. Benigno Mörlin Visconti for the precious collaboration and Dr. Francesco Piovani for the help during sampling and for the useful discussion. Thanks also to Arch. Carlo Capponi and Arch. Laura Lazzaroni, Ufficio Beni Culturali della Diocesi di Milano.

C. Cardell thanks the financial support provided by Spanish Research Projects AERIMPACT (CGL2012-30729) and EXPOAIR (P12-FQM-1889), the European Regional Development Fund (ERDF), and the Andalusian Research Group RNM-179. SEM-EDX analyses were performed in the Scientific Instrumentation Centre (CIC) of the University of Granada.

Appendix A. Supplementary data

Supplementary data to this article can be found online at https://doi.org/10.1016/j.microc.2020.105121.

References

[1] M. Del Monte, C. Sabbioni, O. Vittori, Airborne carbon particles and marble deterioration, Atmos. Environ. 15 (1981) 645–652, https://doi.org/10.1016/0004-6981(81)90269-9.
[2] P. Brimblecombe, History of urban air pollution, in: J. Finger, O. Herter, F. Palmer (Eds). Urban air pollution—European aspects. Kluver, Dordrecht, 1999, pp.7–20.
[3] P. Brimblecombe, Air pollution and architecture, past, present and future, J. Archit. Conserv. 6 (2000) 30–46, https://doi.org/10.1080/13556207.2000.10785268.
[4] A.V. Turkington, B.J. Smith & W.B. Whalley, Short-term stone surface modification; an example from Venice. Proceedings of the 4th international symposium on the conservation of monuments in the Mediterranean basin. Technical chamber of Greece, Rhodes 1, 1997, pp. 359–372.
[5] G. Zappia, C. Sabbioni, C. Riontino, G. Gobbi, O. Favoni, Exposure tests of building materials in urban atmosphere, Sci. Total. Environ. 224 (1998) 235–244, https://doi.org/10.1016/S0048-9697(98)00359-3.
[6] P. Brimblecombe, Environment and architectural stone, in: S. Sigismund, R. Snethlage (Eds.) Stone in architecture, 4th, 461st edn. Springer, Berlin, 2001, pp. 317–346.
[7] N. Ghedini, C. Sabbioni, A. Bonazza, G. Gobbi, Chemical-thermal quantitative methodology for carbon speciation in damage layers on building surfaces, Environ. Sci. Technol. 40 (2006) 939–944, https://doi.org/10.1021/es0501641.
[8] N. Marinoni, M.P. Birelli, C. Rostagno, A. Pavede, The effects of atmospheric multi pollutants on modern concrete, Atmos. Environ. 37 (2003) 4701–4712, https://doi.org/10.1016/j.atmosenv.2003.06.001.
[9] A. Bonazza, C. Sabbioni, N. Ghedini, Quantitative data on carbon fractions in interpretation of black crusts and soiling on European built heritage, Atmos. Environ. 39 (2005) 2607–2618, https://doi.org/10.1016/j.atmosenv.2005.01.040.
[10] C.M. Belfiore, D. Barca, A. Bonazza, V. Comite, M.F. La Russa, A. Pezzino, Application of spectrometric analysis to the identification of pollution sources causing cultural heritage damage, Environ. Sci. Pollut. Res. 20 (2013) 8848–8859, https://doi.org/10.1007/s11356-013-1810-y.
[11] O. Farkas, S. Siegesmund, T. Licha, Á. Török, Geochemical and mineralogical composition of black weathering crusts on limestones from seven different European countries, Environ. Earth Sci. 77 (2018) 211, https://doi.org/10.1007/s12665-018-7384-8.
[12] C. Rodriguez-Navarro, E. Sebastian, Role of particulate matter from vehicle exhaust on porous building stone (limestone) sulfation, Sci. Total. Environ. 187 (1996) 79–91, https://doi.org/10.1016/0048-9697 (96)05124-8.
[13] M.D. Geller, L. Ntziachristos, A. Athanasios Mamakos, Z. Zissis Samaras, D.A. Schmitz, J.R. Froines, C. Sioutas, Physicochemical and redox characteristics of particulate matter (PM) emitted from gasoline and diesel passenger cars, Atmos. Environ. 40 (2006) 6988–7004, https://doi.org/10.1016/j.atmosenv.2006.06.018.
[14] D. Contini, A. Gambaro, F. Belosi, S. De Pieri, W.R.L. Cairns, A. Donateo, E. Zanotto, M. Citron, The direct influence of ship traffic on atmospheric PM2.5, PM10 and

PAH in Venice, J. Environ. Management 92 (2011) 2119–2129, https://doi.org/10.1016/j.jenvman.2011.01.016.
[15] R. Prikryl, J. Svabodová, K. Zák, D. Hradil, Anthropogenic origin of salt crusts on sandstone sculptures of Prague's Charles Bridge (Czech Republic). Evidence of mineralogy and stable isotope geochemistry, Eur. J. Mineral. 16 (2004) 609–618, https://doi.org/10.1127/0935-1221/2004/0016-0609.
[16] K. Torfs, R.E. Van Grieken, F. Buzek, Use of stable isotope measurements to evaluate the origin of sulfur in gypsum layers on limestone buildings, Environ. Sci. Pollut. Res. 31 (1997) 2650–2655, https://doi.org/10.1021/es970067v.
[17] J.M. Vallet, C. Gosselin, P. Bromblet, P. Rolland, V. Vergés-Belmin, W. Kloppmann, Origin of salts in stone monuments degradation using sulphur and oxygen isotopes: first results of the Bourges Cathedral (France), J. Geochem. Explor. 88 (2006) 358–362, https://doi.org/10.1016/j.gexplo.2005.08.075.
[18] J. Schweigstillová, R. Prikryl, M. Novotná, Isotopic composition of salt efflorescence from the sandstone castellated rocks of the Bohemian Cretaceous Basin (Czech Republic), Environ. Geol. 58 (2009) 217–225, https://doi.org/10.1007/s00254-008-1510-y.
[19] N. Schleicher, C. Recio, Source identification of sulphate forming salts on sandstones from onuments in Salamanca, Spain—a stable isotope approach, Environ. Sci. Pollut. Res. 17 (2010) 770–778, https://doi.org/10.1007/s11356-009-0196-3.
[20] W. Kloppmann, P. Bromblet, J.M. Vallet, V. Vergès-Belmin, O. Rolland, C. Guerrot, Building mateials as intrinsic sources of sulphate: a hidden face of salt weathering of historical monuments investigated through multi-isotope tracing (B, O, S), Sci. Total. Environ. 409 (9) (2011) 1658–1669, https://doi.org/10.1016/j.scitotenv.2011.01.008.
[21] S. Kramar, B. Mirtič, K. Knöller, N. Rogan-Šmuc, Weathering of the black limestone of historical monuments (Ljubljana, Slovenia): oxygen and sulfur isotope composition of sulfate salts, Appl. Geochem. 26 (9–10) (2011) 1632–1638, https://doi.org/10.1016/j.apgeochem.2011.04.020.
[22] T. Rivas, S. Pozo, M. Paz, Sulphur and oxygen isotope analysis to identify sources of sulphur in gypsum-rich black crusts developed on granites, Sci. Tot. Environ. 482–483 (2014) 137–147, https://doi.org/10.1016/j.scitotenv.2014.02.128.
[23] D. Barca, V. Comite, C.M. Belfiore, A. Bonazza, M.F. La Russa, S.A. Ruffolo, G.M. Crisci, A. Pezzino, C. Sabbioni, Impact of air pollution in deterioration of carbonate building materials in Italian urban environments, Appl. Geochem. 48 (2014) 122–131, https://doi.org/10.1016/j.apgeochem.2014.07.002.
[24] M.F. La Russa, P. Fermo, V. Comite, C.M. Belfiore, D. Barca, A. Cerioni, M. De Santis, L.F. Barbagallo, M. Ricca, S.A. Ruffolo, The Oceanus statue of the Fontana di Trevi (Rome): the analysis of black crust as a tool to investigate the urban air pollution and its impact on the stone degradation, Sci. Tot. Environ. 593–594 (2017) 297–309, https://doi.org/10.1016/j.scitotenv.2017.03.185.
[25] D. Barca, C.M. Belfiore, G.M. Crisci, M.F. La Russa, A. Pezzino, S.A. Ruffolo, Application of laser ablation ICP-MS and traditional techniques to the study of black crusts on building stones: a new methodological approach, Environ. Sci. Pollut. Res. 17 (2010) 1433–1447, https://doi.org/10.1007/s11356-010-0329-8.
[26] N. Prieto-Taboada, M. Maguregui, I. Martinez-Arkarazo, M.A. Olazabal, G. Arana, J.M. Madariaga, Spectroscopic evaluation of the environmental impact on black crusted modern mortars in urban–industrial areas, Anal. Bioanal. Chem. 399 (2011) 2949–2959, https://doi.org/10.1007/s00216-010-4324-1.
[27] N. Schiavon, G. Chiavari, D. Fabbri, Soiling of limestone in an urban environment characterized by heavy vehicular exhaust emissions, Environ. Geol. 46 (2004) 448–455, https://doi.org/10.1007/s00254-004-1046-8.
[28] H. Morillas, M. Maguregui, C. García-Florentino, J.A. Carrero, J.M. Madariaga, The cauliflower-like black crusts on sandstones: a natural passive sampler to evaluate the surrounding environmental pollution, Environ. Res. 17 (2016) 218–232, https://doi.org/10.1016/j.envres.2016.02.015.
[29] V. Comite, M. Álvarez de Buergo, D. Barca, C.M. Belfiore, A. Bonazza, M.F. La Russa, A. Pezzino, L. Randazzo, S.A. Ruffolo, Damage monitoring on carbonate stones: field exposure tests contributing t, o pollution impact evaluation in two Italian sites, Constr. Buil. Mat. 152 (2017) 907–922, https://doi.org/10.1016/j.conbuildmat.2017.07.048.
[30] V. Comite, P. Fermo, The effects of air pollution on cultural heritage: The case study of Santa Maria delle Grazie al Naviglio Grande (Milan)⋆, Eur. Phys. J. Plus 133 (12) (2018), https://doi.org/10.1140/epjp/i2018-12365-6.
[31] J. Sanjurjo-Sánchez, J.R. Vidal Romaní, C. Alves, Comparative analysis of coatings on granitic substrates from urban and natural settings (NW Spain), Geomorphology 138 (2012) 231–242, https://doi.org/10.1016/j.geomorph.2011.09.008.
[32] J.S. Pozo-Antonio, M.F.C. Pereira, C.S.A. Rocha, Microscopic characterisation of black crusts on different substrates, Sci. Tot. Environ. 584–585 (2017) 291–306, https://doi.org/10.1016/j.scitotenv.2016.12.080.
[33] P. Ausset, M. Del Monte, R.A. Lefèvre, Embryonic sulphated black crusts on carbonate rocks in atmospheric simulation chamber and in the feld: role of carbonaceous fy-ash, Atmos. Environ. 33 (1999) 1525–1534, https://doi.org/10.1016/S1352-2310(98)00399-9.
[34] P. Maravelaki-Kalaitzaki, G. Biscontin, Origin, characteristics and morphology of weathering crusts on Istria stone in Venice, Atmos. Environ. 33 (11) (1999) 1699–1709, https://doi.org/10.1016/S1352-2310(98)00263-5.
[35] A. Bonazza, C. Sabbioni, N. Ghedini, O. Favoni, G. Zappia, Carbon data in black crusts on European monuments, in: C. Saiz- Jimenez (Ed.), Air pollution und cultural heritage, Taylor & Francis, London, 2004, pp. 39–46.
[36] A. Bonazza, C. Sabbioni, N. Ghedini, Quantitative data on car- bon fractions in interpretation of black crusts and soiling on European built heritage, Atmos. Environ. 39 (2005) 2607–2618, https://doi.org/10.1016/j.atmosenv.2005.01.040.
[37] Á. Török, Black crusts on travertine: factors controlling develop- ment and stability, Environ. Geol. 56 (2008) 583–594, https://doi.org/10.1007/s00254-008-1297-x.
[38] M. Urosevic, A. Yebra-Rodríguez, E. Sebastián-Pardo, C. Cardell, Black soiling of an architectural limestone during two-year term exposure to urban air in the city of Granada (S Spain), Sci. Total. Environ. 414 (2012) 564–575, https://doi.org/10.1016/j.scitotenv.2011.11.028.
[39] T. De Kock, J. Van Stappen, G. Fronteau, M. Boone, W. De Boever, F. Dagrain, G. Silversmit, L. Vincze, V. Cnudde, Laminar gypsum crust on lede stone: microspatial characterization and laboratory acid weathering, Talanta 162 (2017) 193–202, https://doi.org/10.1016/j.talanta.2016.10.025.
[40] E. M. Perez-Monserrat, M. J. Varas-Muriel, M. Alvarez De Buergo, R. Fort, Black Layers of Decay and Color Patterns on Heritage Limestone as Markers of Environmental Change, Geosciences (Switzerland) 6(1) (2016) 4. DOI: 10.3390/geosciences6010004.
[41] Monza e la Brianza Editore: Touring Collana: Guide verdi d'Italia, 2006.
[42] R. Cassanelli, Monza anno 1300. La Basilica di S. Giovanni Battista e la sua facciata. Comune di Monza. 1988.
[43] M.F. La Russa, C.M. Belfiore, V. Comite, D. Barca, A. Bonazza, S.A. Ruffolo, G.M. Crisci, A. Pezzino, Geochemical study of black crusts as a diagnostic tool in cultural heritage, Appl. Phys. A Mater. Sci. Process. 113 (2013) 1151–1162, https://doi.org/10.1007/s00339-013-7912-z.
[44] M.F. La Russa, V. Comite, N. Aly, D. Barca, P. Fermo, N. Rovella, F. Antonelli, E. Tesser, M. Aquino, S.A. Ruffolo, Black crusts on Venetian built heritage, investigation on the impact of pollution sources on their composition, Eur. Phys. J. Plus 133 (2018) 370, https://doi.org/10.1140/epjp/i2018-12230-8.
[45] S.A. Ruffolo, V. Comite, M.F. La Russa, C.M. Belfiore, D. Barca, A. Bonazza, G.M. Crisci, A. Pezzino, C. Sabbioni, Analysis of black crusts from the Seville Cathedral: a challenge to deepen understanding the relationship among microstructure, micro chemical features and pollution sources, Sci. Total Environ. 502 (2015) 157–166, https://doi.org/10.1016/j.scitotenv.2014.09.023.
[46] C. R. de Kimpe, Clay and silt analysis, in: M. R. Carter (Eds.), Soil sampling and methods of analysis. Canadian Society of Soil Science, Lewis Publisher; 1993. pp. 719–730.
[47] B. Gratuze, Obsidian characterization by laser ablation ICPMS and its application to prehistoric trade in the Mediterranean and the Near East: sources and distribution of obsidian within the Aegean and Anatolia, J. Archaeol. Sci. 26 (1999) 869–881, https://doi.org/10.1006/jasc.1999.0459.
[48] E. Vander Putten, F. Dehairs, L. André, W. Baeyens, Quantitative in situ microanalysis of minor and trace elements in biogenic calcite using infrared laser ablation-inductively coupled plasma mass spectrometry: a critical evaluation, Anal. Chim. Acta 378 (1999) 261–272, https://doi.org/10.1016/S0003-2670(98)00613-8.
[49] T. Wyndham, M. McCulloch, S. Fallon, C. Alibert, High resolution coral records of rare earth elements in coastal seawater: biogeochemical cycling and a new environmental proxy, Geochim. Cosmochim. Acta 68 (2004) 2067–2080, https://doi.org/10.1016/j.gca.2003.11.004.
[50] D. Barca, C.M. Belfiore, G.M. Crisci, M.F. La Russa, A. Pezzino, S.A. Ruffolo, A new methodological approach for the chemical characterization of black crusts on building stones: a case study from the Catania city centre (Sicily, Italy), J. Anal. At. Spectrom. 26 (2011) 1000–1011, https://doi.org/10.1039/C0JA00226G.
[51] A. Piazzalunga, V. Bernardoni, P. Fermo, R. Vecchi, Optimisation of analytical procedures for the quantification of ionic and carbonaceous fractions in the atmospheric aerosol and applications to ambient samples, Anal. Bioanal. Chem. 405 (2013) 1123–1132, https://doi.org/10.1007/s00216-012-6433-5.
[52] P. Fermo, R. Gonzalez Turrion, M. Rosa, A. Omegna, A new approach to assess the chemical composition of powder deposits damaging the stone surfaces of historical monuments, Environ. Sci. Pollut. Res. 22 (2015) 6262–6270, https://doi.org/10.1007/s11356-014-3855-y.
[53] G. Socrates, Infrared and Raman characteristic group frequencies: Tables and Charts. Chichester: Wiley (Pub.), 2001.
[54] M.D. Lane, Mid-infrared emission spectroscopy of sulfate and sulfate bearing minerals, Am. Miner. 92 (2007) 1–18, https://doi.org/10.2138/am.2007.2170.
[55] N. Schiavon, Kaolinisation of granite in an urban environment, Environ. Geol. 52 (2007) 399–407, https://doi.org/10.1007/s00254-006-0473-0.
[56] D. Gulotta, M. Bertoldi, S. Bortolotto, P. Fermo, A. Piazzalunga, L. Toniolo, The Angera stone: a challenging conservation issue in the polluted environment of Milan (Italy), Environ. Earth. Sci. 69 (2013) 1085–1094, https://doi.org/10.1007/s12665-012-2165-2.
[57] B.J. Saikia, G. Parthasarathy, Fourier transform infrared spectroscopic characterization of kaolinite from assam and meghalaya, North eastern India, J. Mod. Phys. 1 (2010) 206–210.
[58] F. Cappitelli, L. Toniolo, A. Sansonetti, Advantages of using microbial technology over traditional chemical technology in removal of black crusts from stone surfaces of historical monuments, Appl. Environ. Microbiol. 73 (17) (2007) 5671–5675, https://doi.org/10.1128/AEM.00394-07.
[59] D.R. Gentner, G. Isaacman, D.R. Worton, A.W.H. Chan, T.R. Dallmann, L. Davisa, S. Liud, D.A. Day, L.M. Russell, K.R. Wilson, R. Weber, A. Guha, R.A. Harley, A.H. Goldstein, Elucidating secondary organic aerosol from diesel and gasoline vehicles through detailed characterization of organic carbon emissions, Proc. Natl. Acad. Sci. U.S.A. 109 (2012) 18318–18323, https://doi.org/10.1073/pnas.1212272109.
[60] S. Fuzzi, M.O. Andreae, B.J. Hueber, M. Kulmala, T.C. Bon, M. Boy, S.J. Doherty, A. Guenther, M. Kanakidou, K. Kawamura, V.-M. Kerminen, U. Lohmann, L.M. Russell, U. Poschl, Critical assessment of the current state of scientific knowledge, terminology, and research needs concerning the role of organic aerosols in the atmosphere, climate, and global change, Atmos. Chem. Phys. 6 (2006) 2017–2038, https://doi.org/10.5194/acp-6-2017-2006.
[61] I. Vassura, E. Venturini, S. Marchetti, A. Piazzalunga, E. Bernardi, P. Fermo, F. Passarini, Markers and influence of open biomass burning on atmospheric

particulate size and composition during a major bonfire event, Atmos. Environ. 82 (2014) 218–225, https://doi.org/10.1016/j.atmosenv.2013.10.037.
[62] K.R. Daellenbach, C. Bozzetti, A. Křepelová, F. Canonaco, R. Wolf, P. Zotter, P. Fermo, M. Crippa, J.G. Slowik, Y. Sosedova, Y. Zhang, R.-J. Huang, L. Poulain, S. Szidat, U. Baltensperger, I. El Haddad, A.S.H. Prévôt, Characterization and source apportionment of organic aerosol using offline aerosol mass spectrometry, Atmos. Meas. Tech. 9 (1) (2016) 23–39, https://doi.org/10.5194/amt-9-23-2016.
[63] A.L. Robinson, N.M. Donahue, M.K. Shrivastava, E.A. Weitkamp, A.M. Sage, A.P. Grieshop, T.E. Lane, J.R. Pierce, S.N. Pandis, Rethinking organic aerosols: semivolatile emissions and photochemical aging, Science 315 (2007) 1259–1262, https://doi.org/10.1126/science.1133061.
[64] V. Bernardoni, R. Vecchi, G. Valli, A. Piazzalunga, P. Fermo, PM10 source apportionment in Milan (Italy) using time-resolved data, Sci. Tot. Environ. 409 (2011) 4788–4795, https://doi.org/10.1016/j.scitotenv.2011.07.048.
[65] P. Fermo, A. Piazzalunga, R. Vecchi, G. Valli, M. Ceriani, A TGA/FT-IR study for measuring OC and EC in aerosol samples, Atmos Chem Phys 6 (1) (2006) 255–266.
[66] R. Vecchi, V. Bernardoni, P. Fermo, F. Lucarelli, F. Mazzei, S. Nava, P. Prati, A. Piazzalunga, G. Valli, 4-hours resolution data to study PM10 in a “hot spot” area in Europe, Environ. Monit. Assess. 154 (2009) 283–300, https://doi.org/10.1007/s10661-008-0396-1.
[67] R. Rossi Manaresi, Oxalate patinas and conservation treatments, p. 113–127, in: M. Realini and L. Toniolo (Eds.), The oxalate films in the conservation of works of art. Proceedings of the 2nd International Symposium, 25 to 27 March 1996 EDITEAM. Bologna, Italy, 1996, pp. 113–127.
[68] A.E. Charola, R. Ware, Acid deposition and the deterioration of stone: a brief review of a broad topic, Geol. Soc. Spec. Pub. 205 (2002) 393–406, https://doi.org/10.1144/GSL.SP.2002.205.01.28.
[69] T. Hosono, E. Uchida, C. Suda, A. Ueno, T. Nakagawa, Salt weathering of sandstone at the Angkor monuments, Cambodia: identification of the origins of salts using sulphur and strontium isotopes, J. Archaeol. Sci. 33 (2006) 1541–1551, https://doi.org/10.2465/ganko.93.411.
[70] N. Schleicher, C. Recio, Source identification of sulphate forming salts on sandstones from monuments in Salamanca, Spain—a stable isotope approach, Environ. Sci. Pollut. Res. 17 (2010) 770–778, https://doi.org/10.1007/s11356-009-0196-3.
[71] W. Kloppmann, P. Bromblet, J.M. Vallet, V. Vergès-Belmin, O. Rolland, C. Guerrot, Building materials as intrinsic sources of sulphate: a hidden face of salt weathering of historical monuments investigated through multi-isotope tracing (B, O, S), Sci. Total. Environ. 409 (9) (2011) 1658–1669, https://doi.org/10.1016/j.scitotenv.2011.01.008.
[72] J.S. Pozo-Antonio, M.F.C. Pereira, C.S.A. Rocha, I. Puente, C. Figueiredo, Comparative study of deterioration forms on nearby granitic bridges from an urban setting in the NW Iberian Peninsula, Geomorphology 274 (2016) 11–30, https://doi.org/10.1016/j.geomorph.2016.09.009.
[73] M. Del Monte, C. Sabbioni, G. Zappia, The origin of calcium oxalates on histor- ical buildings, monuments and natural out- crops, Sci. Tot. Environ. 67 (1987) 17–39, https://doi.org/10.1016/0048-9697(87)90063-5.
[74] J. Russ, W.D. Kaluarachchi, L. Drummond, H.G.M. Edwards, The Nature of a Whewellite-Rich Rock Crust Associated with Pictographs in Southwestern Texas, J. Stud. Conserv. 44 (2) (1999) 91–103, https://doi.org/10.1179/sic.1999.44.2.91.
[75] P.D. Safai, M.P. Raju, P.S.P. Rao, G. Pandithurai, Characterization of carbonaceous aerosols over the urban tropical location and a new approach to evaluate their climatic importance, Atmos. Environ. 92 (2014) 493–500, https://doi.org/10.1016/j.atmosenv.2014.04.055.
[76] S.M.L. Hamaa, L.R. Cordell, J. Staelens, D. Mooibroek, P.S. Monks, Chemical composition and source identification of PM10 in five North Western European cities, Atmos. Res. 214 (2018) 135–149, https://doi.org/10.1016/j.atmosres.2018.07.014.
[77] J.H. Seinfeld, S.N. Pandis, Chapter 14 Atmospheric Organic Aerosols, In: Atmospheric Chemistry and Physics: From Air Pollution to Climate Change, 3rd Edition (Eds) John Wiley and Sons. Inc., New York. 2006, pp. 573-559.
[78] J. Schauer, M. Kleeman, G. Cass, B. Simoneit, Measurement of emissions from air pollution sources. 1. C1 through C29 organic compounds from meat charbroiling, Environ. Sci. Technol. 33 (10) (1999) 1566–1577.
[79] J.J. Schauer, M.J. Kleeman, G.R. Cass, B.R. Simoneit, Measurement of emissions from air pollution sources. 5. C1–C32 organic compounds from gasoline-powered motor vehicles, Environ. Sci. Technol. 36 (2002) 1169–1180, https://doi.org/10.1021/es0108077.
[80] S. Saarikoski, H. Timonen, K. Saarnio, M. Aurela, L. Jarvi, P. Keronen, V.M. Kerminen, R. Hillamo, Sources of organic carbon in fine particulate matter in northern European urban air, Atmos. Chem. Phys. 8 (2008) 6281–6295, https://doi.org/10.5194/acp-8-6281-2008.
[81] J. Cao, Z. Shen, J.C. Chow, G. Qi, J.G. Watson, Seasonal variations and sources of mass and chemical composition for PM10 aerosol in Hangzhou, China, Particuology 7 (2009) 161–168, https://doi.org/10.1016/j.partic.2009.01.009.
[82] D. Camuffo, M. Del Monte, C. Sabbioni, Influenza delle precipitazioni e della condensazione sul degrado superficiale dei monumenti in marmo e calcare. Materiali Lapidei. Volume Speciale del Bollettino, Roma, p.15-36, 1987.
[83] C. Sabbioni, G. Zappia, Oxalate patinas on ancient monument: the biological hypothesis, Aerobiol. Issue 7 (1991) 31–37, https://doi.org/10.1007/BF02450015.
[84] C. Sabbioni, Contribution of atmospheric deposition to the formation of damage layers, Sci. Total. Environ. 167 (1995) 49–55, https://doi.org/10.1016/0048-9697(95)04568.
[85] A. Bonazza, P. Brimblecombe, C.M. Grossi, C. Sabbioni, Carbon in black crust from the tower of London, Environ. Sci. Technol. 41 (2007) 4199–4204, https://doi.org/10.1021/es062417w.
[86] D. Gulotta, F. Villa, F. Cappitelli, L. Toniolo, Biofilm colonization of metamorphic lithotypes of a renaissance cathedral exposed to urban atmosphere, Sci. Tot. Environ. 639 (2018) 1480–1490, https://doi.org/10.1016/j.scitotenv.2018.05.277.
[87] R. Vecchi, M. Chiari, A. D’Alessandro, P. Fermo, F. Lucarelli, F. Mazzei, S. Nava, A. Piazzalunga, P. Prati, F. Silvani, G. Valli, A mass closure and PMF source apportionment study on the sub-micron sized aerosol fraction at urban sites in Italy, Atmos. Environ. 42 (2008) 2240–2253, https://doi.org/10.1016/j.atmosenv.2007.11.039.
[88] C. Saiz-Jimenez, Air pollution and Cultural Heritage. Proceedings of the International, Workshop on Air Pollution and Cultural Heritage, Seville, Spain, 2003.
[89] C. Perrino, S. Canepari, M. Catrambone, S. Dalla Torre, E. Rantica, T. Sargolini, Influence of natural events on the concentration and composition of atmospheric particulate matter, Atmos. Environ. 43 (2009) 4766–4779, https://doi.org/10.1016/j.atmosenv.2008.06.035.
[90] S. Sandrini, S. Fuzzi, A. Piazzalunga, P. Prati, P. Bonasoni, F. Cavalli, M.C. Bove, M. Calvello, D. Cappelletti, C. Colombi, D. Contini, G. De Gennaro, A. Di Gilio, P. Fermo, L. Ferrero, V. Gianelle, M. Giugliano, P. Ielpo, G. Lonati, A. Marinoni, D. Massabò, U. Molteni, B. Moroni, G. Pavese, C. Perrino, M.G. Perrone, M.R. Perrone, Spatial and seasonal variability of carbonaceous aerosol across Italy, Atmos. Environ. 99 (2014) 587–598, https://doi.org/10.1016/j.atmosenv.2014.10.032.
[91] C. Colombi, Relazione Campagna PoAIR febbraio 2014. Available online: http://www.arpalombardia.it/qariafiles/varie/Relazione%20campagna%20PoAIR%20febbraio%202014.pdf (accessed on 5 August 2019).
[92] EEA Report No 1/2017. Climate change, impacts and vulnerability in Europe 2016 An indicator-based report. European Environment Agency. Luxembourg: Publications Office of the European Union, 2017.
[93] M.D. Geller, L. Ntziachristos, A. Athanasios Mamakos, Z. Zissis Samaras, D.A. Schmitz, J.R. Froines, C. Sioutas, Physicochemical redox characteristics of particulate matter (PM) emitted from gasoline and diesel passenger cars, Atmos. Environ. 40 (2006) 6988–7004, https://doi.org/10.1016/j.atmosenv.2006.06.018.
[94] J. Sternbeck, A. Sjödin, K. Andréasson, Metal emissions from road traffic and the influence of resuspension results from two tunnel studies, Atmos. Environ. 36 (2002) 4735–4744, https://doi.org/10.1016/S1352-2310(02)00561-7.
[95] G. Dongarrà, E. Manno, D. Varrica, Possible markers of traffic-related emissions, Environ. Monit. Assess. 154 (2009) 117–125, https://doi.org/10.1007/s002549900071.
[96] H. Harmens, D.A. Norris, G.R. Koerber, A. Buse, E. Steinnes, A. Rühling, Temporal trends in the concentration of arsenic, chromium, copper, iron, nickel, vanadium and zinc in mosses across Europe between 1990 and 2000, Atmos. Environ. 31 (2007) 6673–6687, https://doi.org/10.1016/j.atmosenv.2007.03.062.
[97] H. Harmens, D.A. Norris, the participants of the moss survey, Spatial and temporal trends in heavy metal accumulation in mosses in Europe (1990–2005). Programme Coordination Centre for the ICP Vegetation, Centre for Ecology & Hydrology. Bangor, UK, Natural Environment Research Council, 2008.